# Electronic Supplementary Information

## Timing matters: pre-assembly versus post-assembly functionalization of a polyoxovanadate–organic cuboid

Ji Guo,[a] Junrui Liu,[b] Yingcui Cui,[a] Chuanhong Liu,[a] Yangming Wang,[a] Mou Wang,[a] Danmeng Huang,[a] Guanying Chen,[a] Wei Wang,*[b] Debin Xia,[a] and Xikui Fang*[a]

[a] *MIIT Key Laboratory of Critical Materials Technology for New Energy Conversion and Storage, School of Chemistry and Chemical Engineering, Harbin Institute of Technology, Harbin 150001, China. E-mail: xkfang@hit.edu.cn*

[b] *CAS Key Laboratory of Design and Assembly of Functional Nanostructures, and Fujian Provincial Key Laboratory of Nanomaterials, Fujian Institute of Research on the Structure of Matter, Chinese Academy of Sciences; Xiamen Institute of Rare Earth Materials, Haixi Institutes, Chinese Academy of Sciences, Xiamen, Fujian, 361021, China. E-mail: wangwei@fjirsm.ac.cn*

## Table of Contents

**Materials and Syntheses**.....S2
**Instruments and Physical Measurements** .....S3
Infrared spectra (Fig. S1) .....S4
Thermogravimetric analyses (Figs. S2–S4) .....S4
Adsorption of dye molecules (Figs. S5–S8).....S6
$^{1}$H and $^{31}$P NMR spectra of **1**, **1'** and **2** (Figs. S9–S13) .....S9
ESI-MS spectra of **1** showing the steps of lossing each methyl radical (Fig. S14).....S11
XPS spectra of **1**, **1'** and **2** (Figs. S15–S17).....S12
Additional NMR spectra (Figs. S18–S21) .....S13
**Single-Crystal X-Ray Structure Determination** .....S15
Crystal data for **1** (Table S1) .....S15
Crystal data for **1'** (Table S2).....S16
Crystal data for **2** (Table S3) .....S17
The distances between adjacent SBUs and those between QPTC linkers (Fig. S22–S23).....S18
The interior void space of **1**, **1'** and **2** (Fig. S24) .....S19
The channel space between molecules in the packing diagrams of **1**, **1'** and **2** (Fig. S25).....S20
**Bond Valence Sum (BVS) Calculations**(Table S4–S7) .....S21
**References** .....S25

## Materials and Syntheses

**Materials:** All reagents were from Innochem (Beijing), TCI Co., Sigma-Aldrich, Acros, and Fisher Chemical, and used without further purification. The synthesis of quaterphenyl-3,3’’’,5,5’’’-tetracarboxylic acid ($H_4$QPTC) was conducted by following a reported procedure.[S1]

**$TMA_{10}\{[(V^{IV}_6O_6)(OCH_3)_9(SO_4)]_8(QPTC)_8[V^{V}_3O_3(OH)_2(H_2O)_3]_2\}\cdot 18CH_3OH\cdot 23DMF$ ($TMA_{10}$·1·$18CH_3OH$·23DMF):**

$VOSO_4\cdot 5H_2O$ (0.06 g, 0.24 mmol) and $H_4$QPTC (0.02 g, 0.04 mmol) were suspended in a 3 mL mixture of DMF:MeOH (1:2 v/v), then the mixture was placed in a Parr Teflon-lined stainless steel vessel and heated at 150 °C. After 3 days, green prismatic crystals were obtained (yield 0.02 g, 33.0% based on V). Elemental analysis, calcd.: C, 37.3%; H, 5.2%; N, 3.4%; S, 1.9%; V, 20.2%; found: C, 38.0%; H, 5.2%; N, 3.8%; S, 2.1%; V, 21.3%. IR (2% KBr pellet, 4000–400 $cm^{-1}$): 3447(br), 2926(w), 2819(w), 1615(w), 1574(s), 1488(w), 1438(w), 1381(w), 1223(w), 1073(w), 949(vs), 772(w), 721(w), 650(w), 575(w), 541(s).

**$TMA_{20}\{[(V^{IV}_6O_6)(OCH_3)_9(C_6H_5PO_3)]_8(QPTC)_8[(V^{IV}_2O_2(OCH_3)_2]_2\}\cdot 17CH_3OH\cdot 6DMF$ ($TMA_{20}$·1’·$17CH_3OH$·6DMF):**

The crystals of complex **1** (0.02 g, 0.0015 mmol) and phenylphosphonic acid (0.002 g, 0.012 mmol) were suspended in a 3 mL mixture of DMF:MeOH (1:2 v/v), then the mixture was placed in a Parr Teflon-lined stainless steel vessel and heated at 150 °C. After 3 days, green prismatic crystals were obtained (yield 0.01 g, 50.9% based on V). Elemental analysis, calcd.: C, 41.6%; H, 5.5%; N, 2.7%; P, 1.9%; V, 19.8%; found: C, 39.8%; H, 5.8%; N, 2.7%; P, 2.2%; V, 21.0%. IR (2% KBr pellet, 4000–400 $cm^{-1}$): 3447(br), 3034(w), 2926(w), 2818(w), 1663(s), 1614 (s), 1573(s), 1487(w), 1438(s), 1419(s), 1381(w), 1226(w), 1072(s), 948(vs), 772(w), 721(w), 650(w), 563(w), 541(w).

**$TMA_{16}\{[(V^{IV}_6O_6)(OCH_3)_9(C_6H_5PO_3)]_8(QPTC)_2(HQPTC)_4(H_2QPTC)_2\}\cdot 15CH_3OH\cdot 13DMF$ ($TMA_{16}$·2·$15CH_3OH$·13DMF):**

$VOSO_4\cdot 5H_2O$ (0.06 g, 0.24 mmol), $H_4$QPTC (0.02 g, 0.04 mmol) and phenylphosphonic acid (0.01 g, 0.06 mmol) were suspended in a 3 mL mixture of DMF:MeOH (1:2 v/v), then the mixture was placed in a Parr Teflon-lined stainless steel vessel and heated at 150 °C for 3 days. After slow cooling to room temperature, green plate crystals were obtained (yield 0.03 g, 45.6% based on V). Elemental analysis, calcd.: C, 42.2%; H, 5.5%; N, 3.1%; P, 1.9%; V, 18.6%; found: C, 43.1%; H, 5.9%; N, 3.2%; P, 1.9%; V, 17.8%. IR (2% KBr pellet, 4000–400 $cm^{-1}$): 3446(br), 3030(w), 2923(w), 2814(w), 1725(w), 1667 (s), 1613(w), 1573(s), 1488(w), 1443(w), 1417(w), 1380(w), 1317(w), 1246(w), 1134(w), 1070(vs), 947(vs), 764(w), 722(w), 564(vs).

## Instruments and Physical Measurements

**General:** IR spectra (KBr pellets) were collected on a Thermo Nicolet Avatar 360 FTIR spectrophotometer. Atmosphere compensation ($CO_2$ and $H_2O$) and baseline corrections were carried out after spectrum collection. $^{1}H$ NMR spectra and $^{31}P$ NMR were collected on a Bruker Avance III 400 MHz NMR instrument. For base-digestion NMR experiments, the MOP samples were dissolved in 1 M NaOD and aged for 2 days (or until the solution turned colorless, indicating complete oxidation of V(IV) to V(V)) before running NMR measurements. Elemental analyses were performed on a Vario EL III analyzer (for C, H, N) and Perkin-Elmer ICP–OES (for P, S, and V). The UV-visible spectra were recorded on a Perkin-Elmer Lambda 750 spectrophotometer. Thermal gravimetric analyses were measured with a TA Instruments SDT-Q600 thermal analysis system under $N_2$ flow with 10 °C/min heating. High-resolution mass spectra were obtained on a quadrupole-orbitrap mass spectrometer (QExactive, ThermoFisher Scientific). The mobile phase consisted of (A) Milli-Q water and (B) HPLC-grade acetonitrile. The HPLC-MS was operated with electrospray ionization in negative polarity mode. The solvent molecules, especially those between MOP cages, are highly disordered in the crystal structures. Therefore, the numbers of the solvent molecules ($CH_3OH$ and DMF) were determined by TGA and elemental analyses.

The determination of counter ions (both their identities and numbers) in the three MOP compounds was based on collective evidence from single-crystal X-ray diffraction, NMR spectroscopy, TGA, and elemental analyses. Solvothermal decomposition of DMF solvents has been known to generate dimethylammonium ($DMA^+$) and tetramethylammonium ($TMA^+$) ions, depending on the reaction conditions and if other solvents such as $CH_3OH$ are also present.[S2, S3] In each of the MOP crystal structures, we have located multiple $TMA^+$ counter ions. Solution NMR in DMSO-$d_6$, although no informative for identifying the ligand signals, can exclude the presence of $DMA^+$ in the crystals as there is no peaks at 2.47 and 9.08 ppm (from internal $DMA^+Cl^-$ reference). The $TMA^+$ signals, however, overlap with that of the methoxide groups on the {$V_6$S/P} SBUs (See Figs. S20 and S21). Thermal decomposition of $TMA^+$ counterions in TGA occurs in the temperature range of 375–550 °C as a well-separated weight loss step, so its number can be accurately determined.

**Single-crystal X-ray diffraction**: The single-crystal X-ray diffraction data were collected using a Bruker D8 Quest X-ray diffractometer equipped with an Incoatec Microfocus Mo Source (I$\mu$S 3.0, $\lambda$ = 0.71071 Å) and a PHOTON II CPAD detector. Suitable crystals were coated with Paratone N oil, suspended on a small fiber loop, and placed in a 173(2) K cooled nitrogen stream from Oxford Cryosystems Cryostream equipment. For all cases, the raw data were processed with the Bruker APEX3 software package. The data were solved by intrinsic phasing methods[S4] and the refinement was done by full-matrix least squares on $F^2$ using SHELXL[S5] (2018/3). Hydrogen atoms on the organic linkers, terminal methoxyl groups, the interior organophosphonate units and the tetramethylammonium counter ions are place geometrically and refined using a riding model; FLAT and AFIX 66 restraints were used, if necessary, to treat the disordered phenyl groups on the phosphonates and organic linkers (QPTC). The SQUEEZE option of PLATON[S6] was used to model the contribution of disordered solvent molecules and counter ions to the reflection intensities.

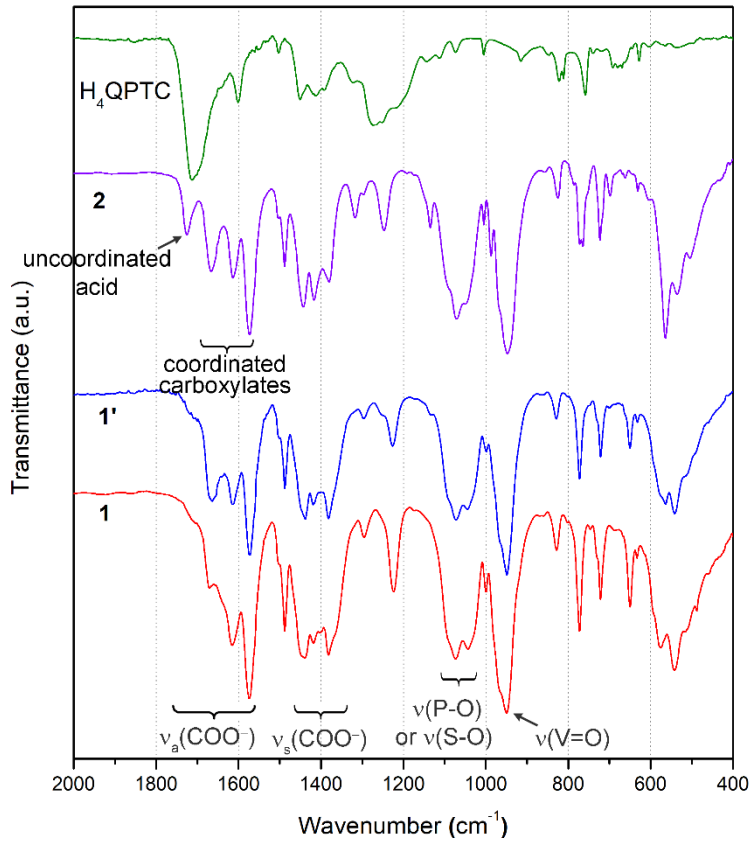


**Fig. S1**. Comparison of the IR spectra of $H_4$QPTC, **1**, **1'** and **2**.

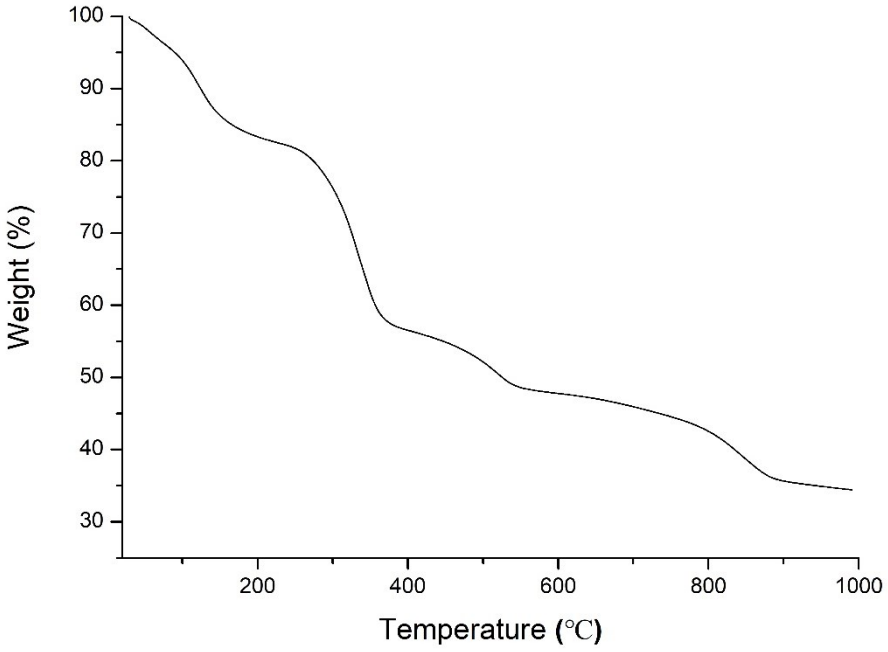


**Fig. S2**. Thermogravimetric analysis trace of **1**. The weight loss of 4.1% between 30 and 80 °C is associated with the loss of c.a. 18 methanol molecules (calcd. 4.2%); the weight loss of 12.5% between 80 and 200 °C is associated with the loss of c.a. 23 N, N-dimethylformamide molecules (calcd. 12.3%).

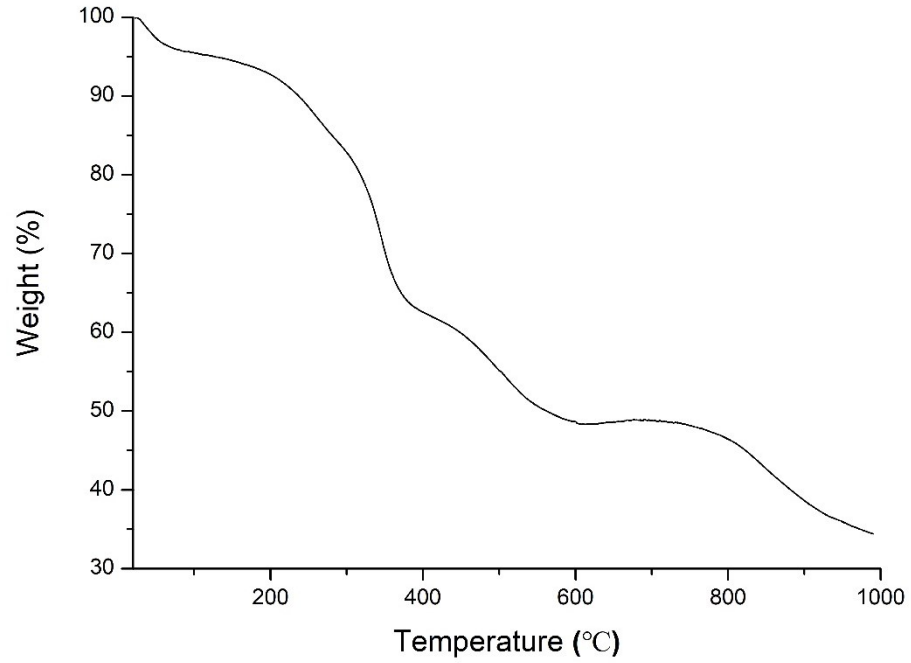


**Fig. S3**. Thermogravimetric analysis trace of **1'**. The weight loss of 4.1% between 30 and 80 °C is associated with the loss of c.a. 17 methanol molecules (calcd. 4.1%); the weight loss of 3.1% between 80 and 200 °C is associated with the loss of c.a.6 N, N-dimethylformamide molecules (calcd. 3.2%).

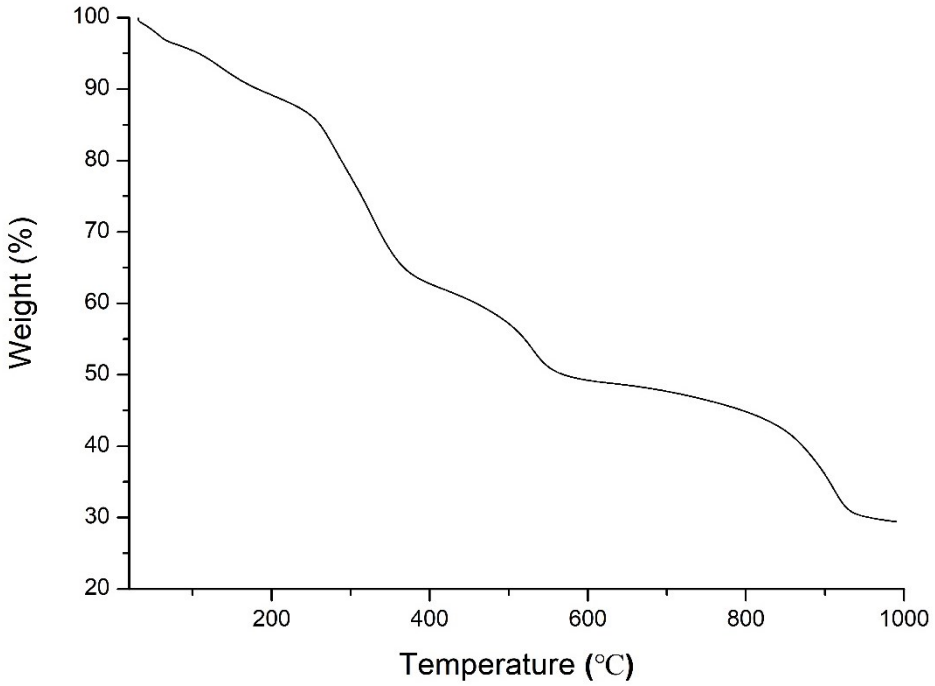


**Fig. S4**. Thermogravimetric analysis trace of **2**. The weight loss of 3.8% between 30 and 80 °C is associated with the loss of c.a. 15 methanol molecules (calcd. 3.7%); the weight loss of 7.0% between 80 and 200 °C is associated with the loss of c.a. 13 N, N-dimethylformamide molecules (calcd. 7.2%).

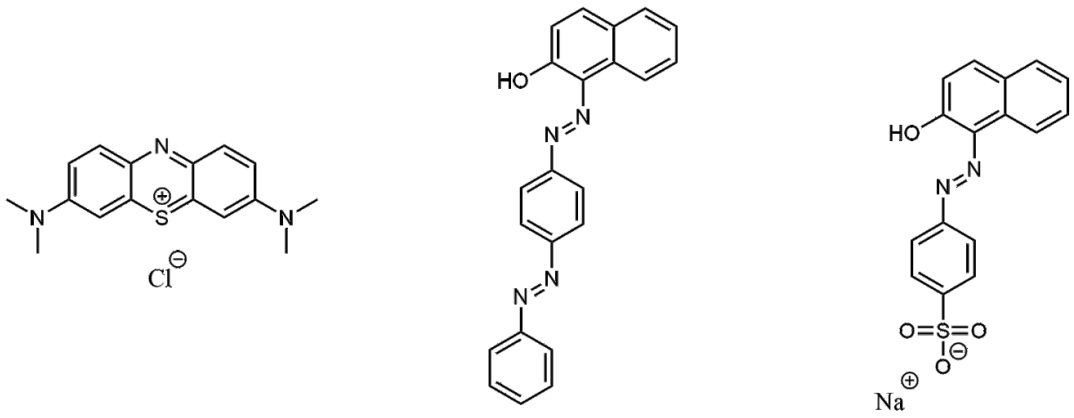


**Fig. S5**. The dye molecules that were used for absorption studies in this work .

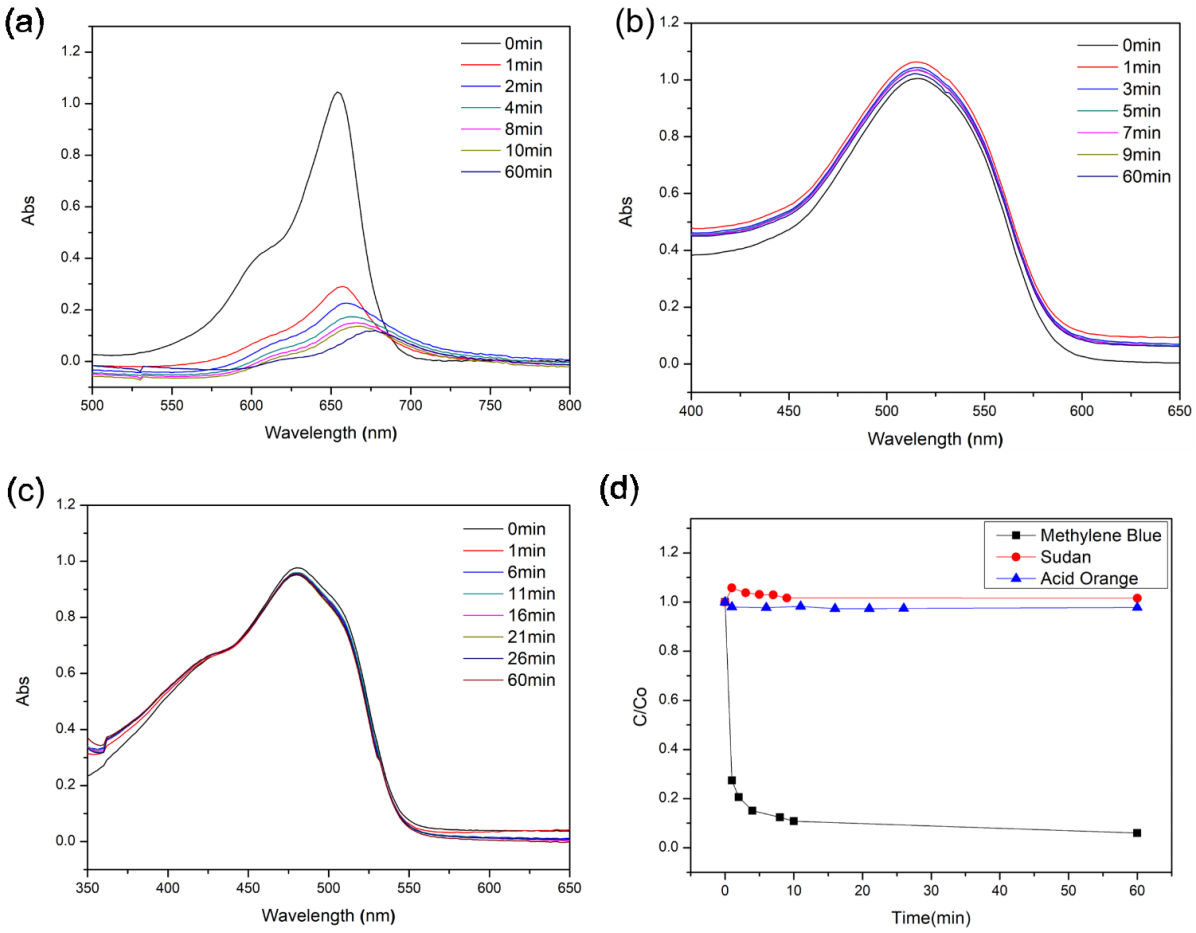


**Fig. S6**. Adsorption of dye molecules by **1**. Temporal evolution of the UV–Vis absorption spectra of $MB^+$ ($1.25\times10^{-5}$ M, 4 mL, a), SD ($1.25\times10^{-4}$ M, 4 mL, b) and $AO^-$ ($6.25\times10^{-5}$ M, 4 mL, c) in ethanol solution with 2 mg of compound **1**. (d) Dye adsorption monitored through the decrease in absorbance at selected wavelengths ($MB^+$: 652 nm; SD: 515 nm; $AO^-$: 480 nm).

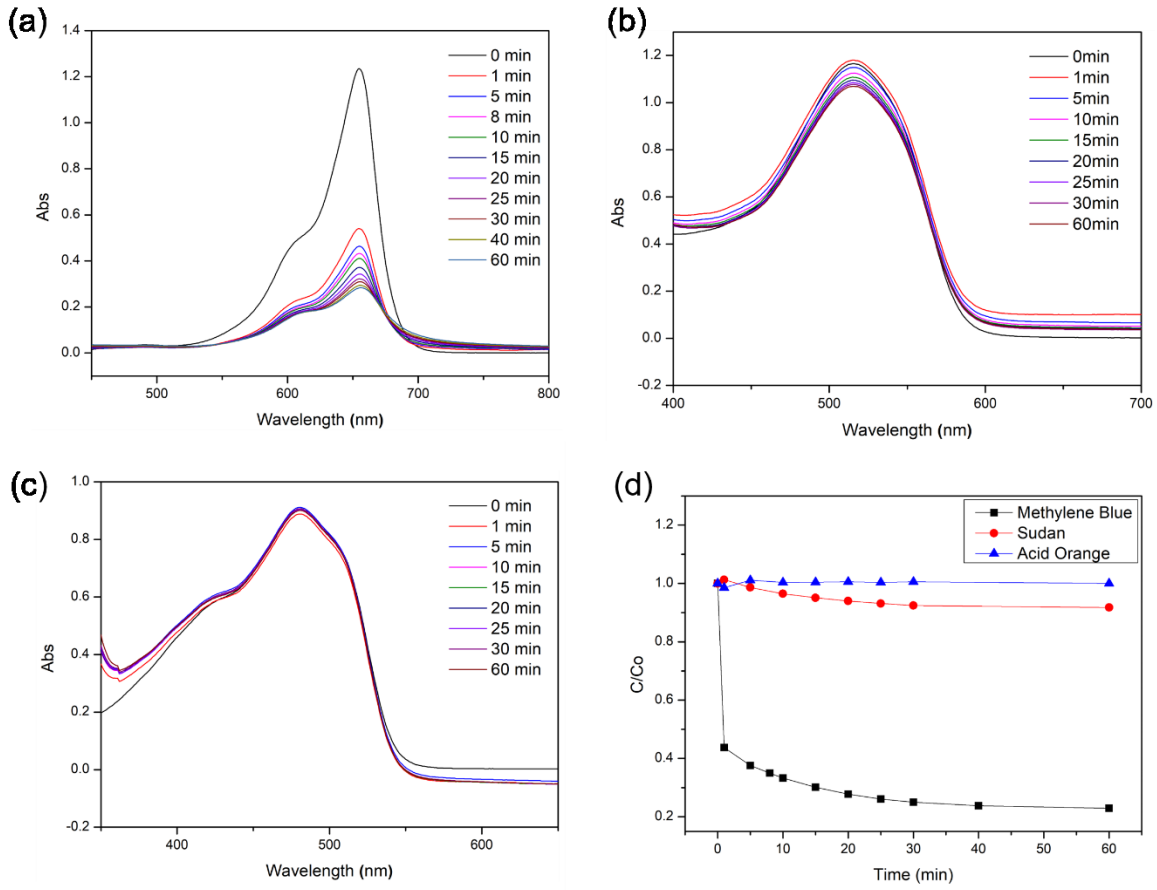


**Fig. S7**. Adsorption of dye molecules by **1'**. Temporal evolution of the UV–Vis absorption spectra of $MB^+$ ($1.25\times10^{-5}$ M, 4 mL, a), SD ($1.25\times10^{-4}$ M, 4 mL, b) and $AO^-$ ($6.25\times10^{-5}$ M, 4 mL, c) in ethanol solution with 2 mg of compound **1'**. (d) Dye adsorption monitored through the decrease in absorbance at selected wavelengths ($MB^+$: 652 nm; SD: 515 nm; $AO^-$: 480 nm).

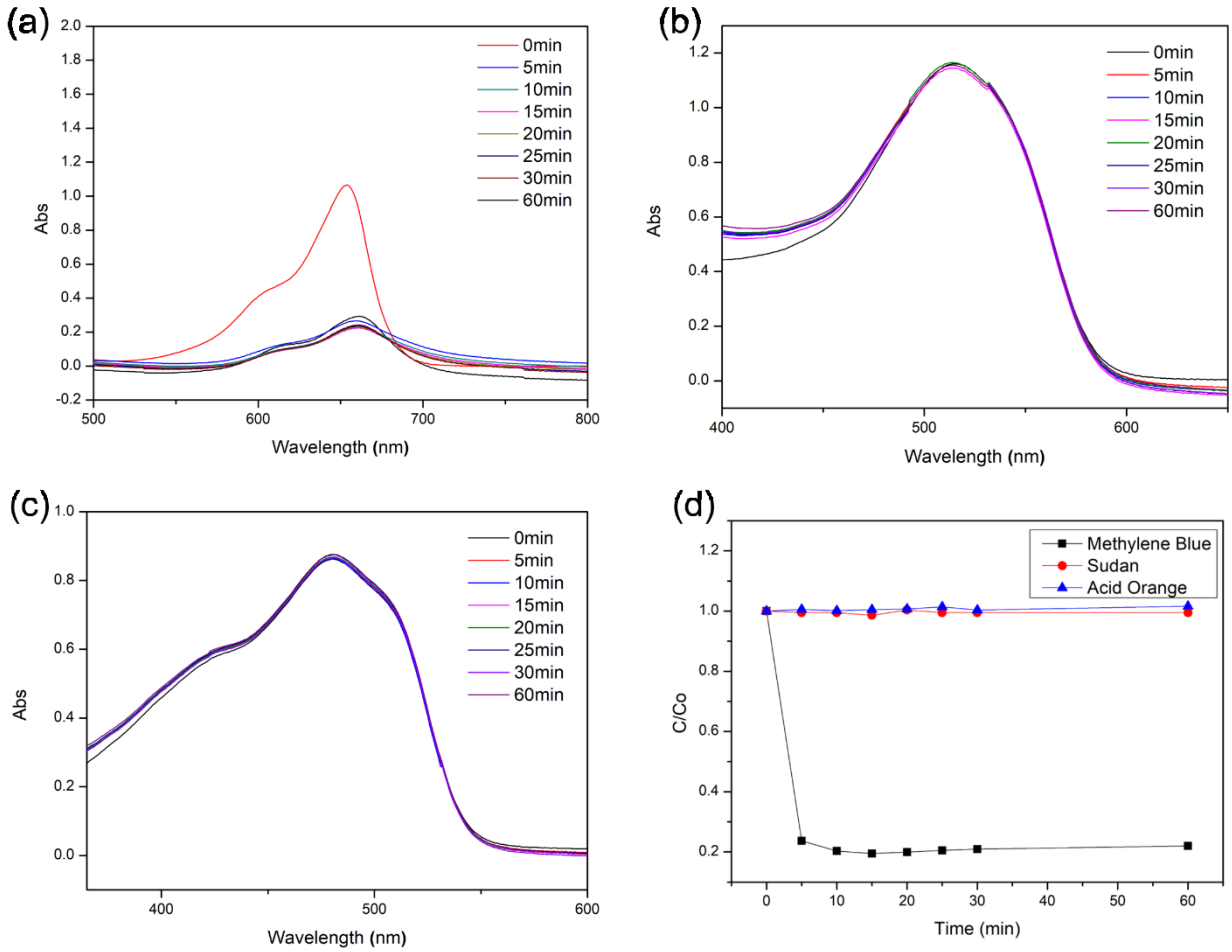


**Fig. S8**. Adsorption of dye molecules by **2**. Temporal evolution of the UV–Vis absorption spectra of $MB^+$ ($1.25\times10^{-5}$ M, 4 mL, a), SD ($1.25\times10^{-4}$ M, 4 mL, b) and $AO^-$ ($6.25\times10^{-5}$ M, 4 mL, c) in ethanol solution with 2 mg of compound **2**. (d) Dye adsorption monitored through the decrease in absorbance at selected wavelengths ($MB^+$: 652 nm; SD: 515 nm; $AO^-$: 480 nm).

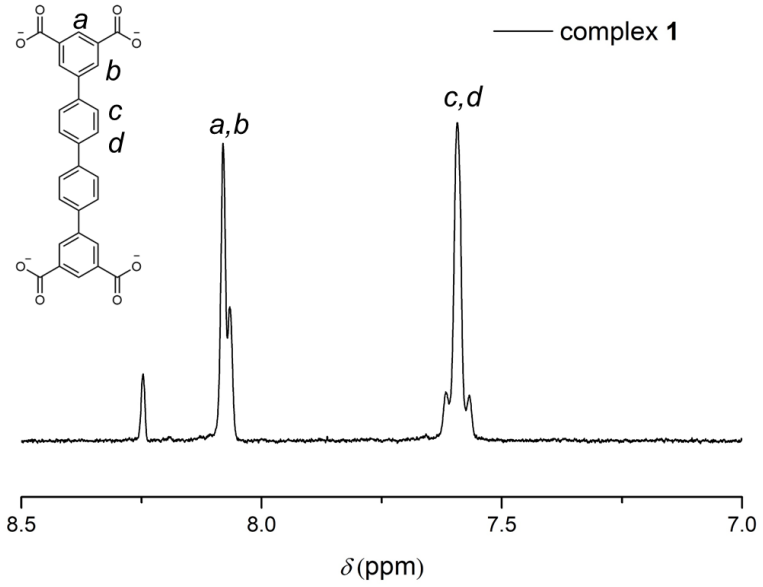


**Fig. S9**. [1]H NMR spectrum of a base-digested sample of **1** (400 MHz, NaOD/$D_2O$, 293 K).

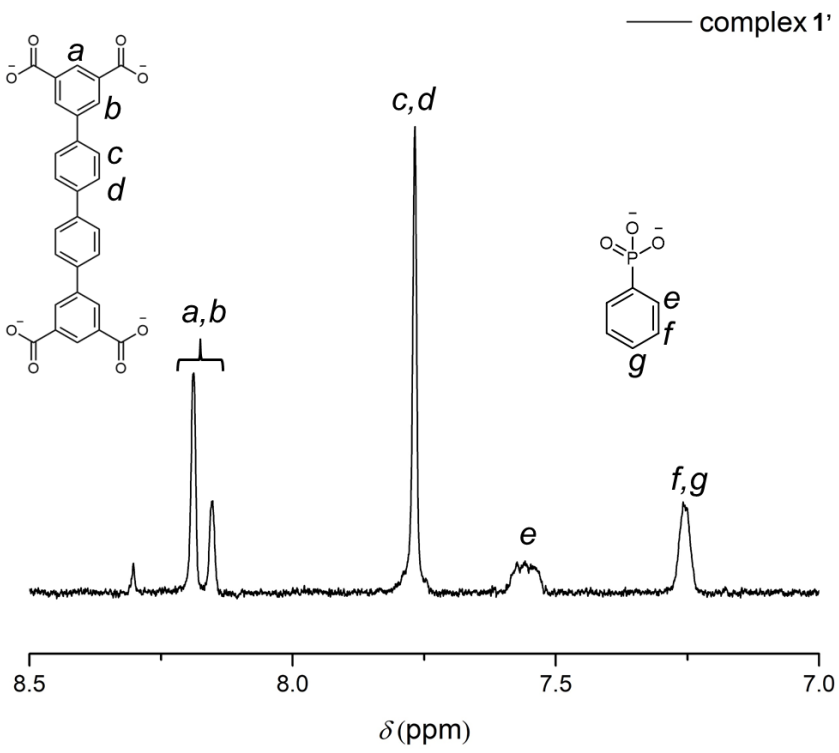


**Fig. S10**. [1]H NMR spectrum of a base-digested sample of **1'** (400 MHz, NaOD/$D_2O$, 293 K)

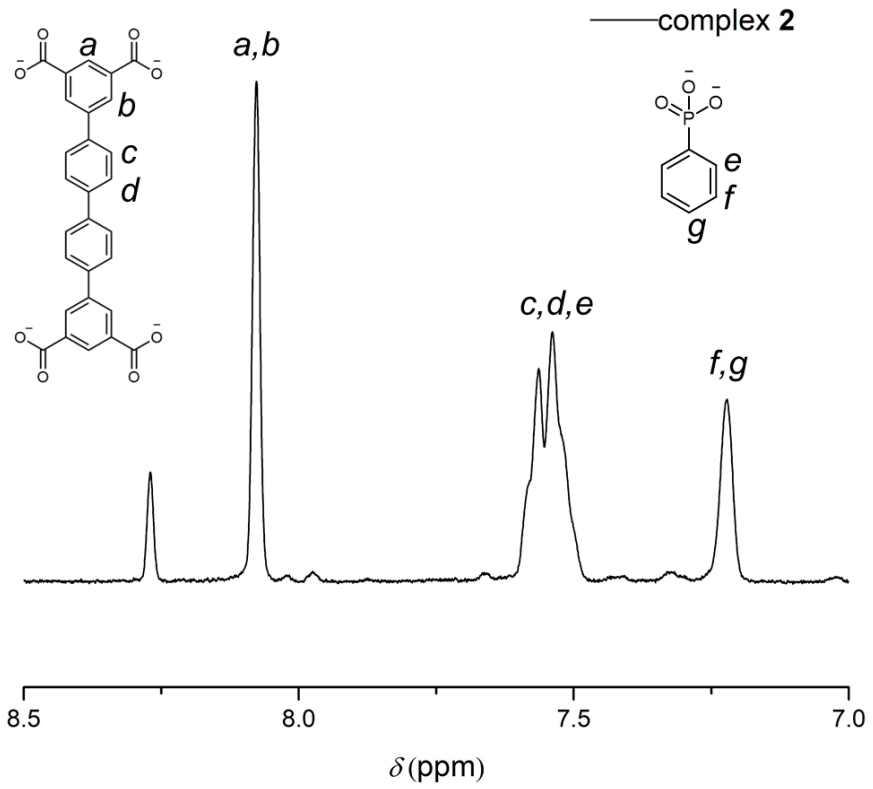


**Fig. S11**. $^{1}$H NMR spectrum of a base-digested sample of **2** (400 MHz, NaOD/$D_2O$, 293 K)

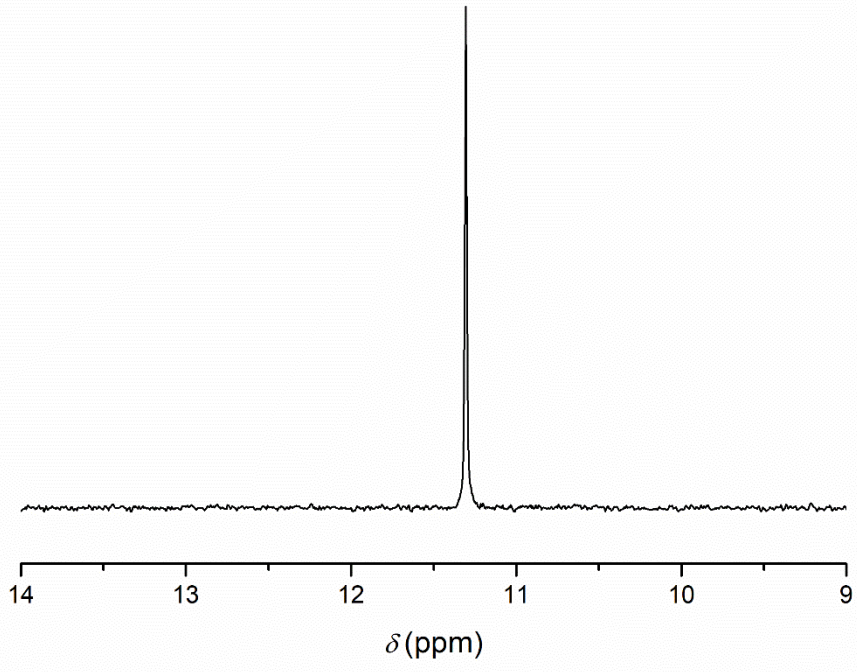


**Fig. S12**. $^{31}$P NMR spectrum of a base-digested sample of **1'** (400 MHz, NaOD/$D_2O$, 293 K)

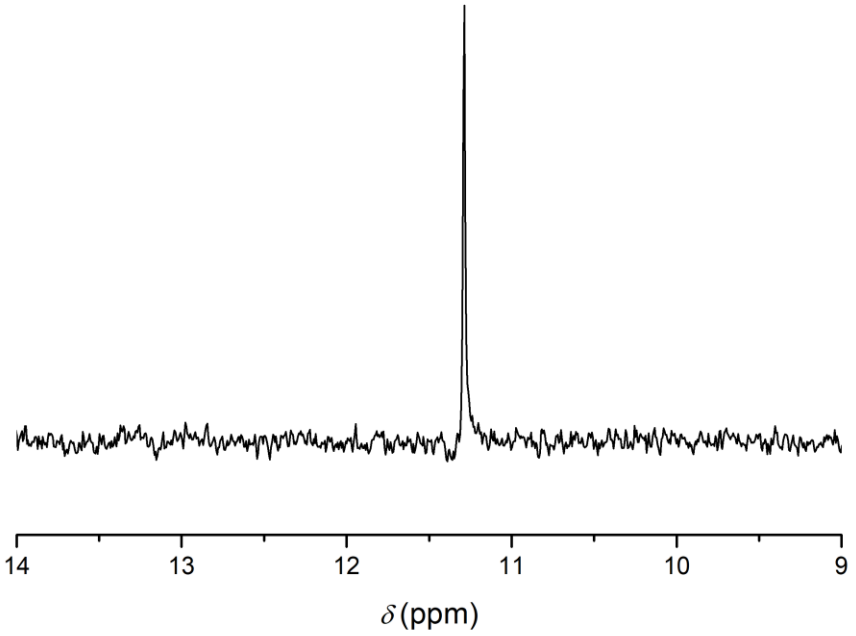


**Fig. S13**. $^{31}$P NMR spectrum of a base-digested sample of **2** (400 MHz, NaOD/$D_2O$, 293 K)

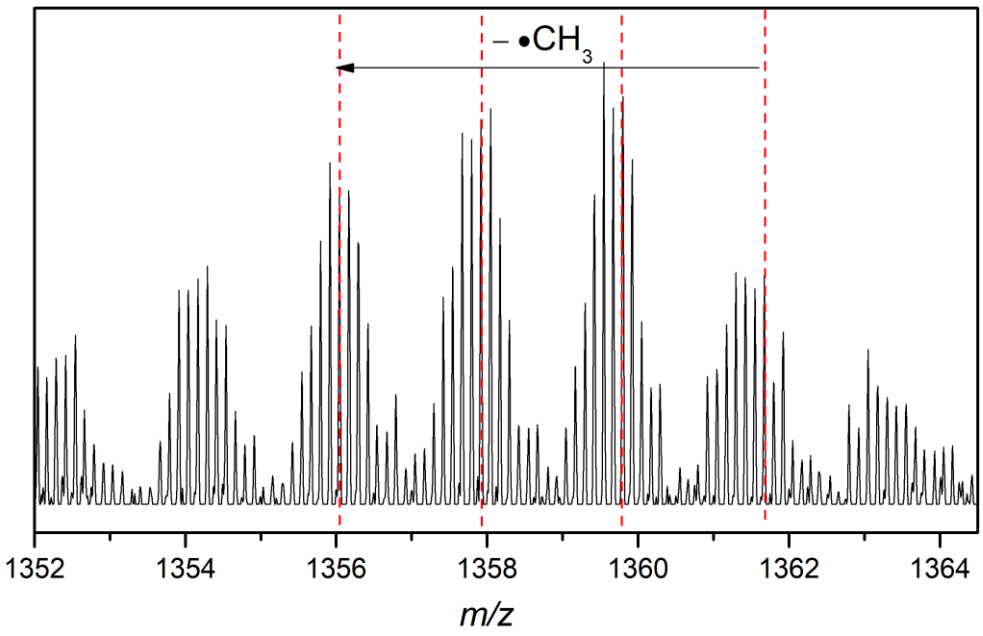


**Fig. S14**. Mass spectrum of compound **1** in the *m/z* range of 1352–1364 (8− charge state); each adjacent envelope of peaks differs by that of a methyl radical (15 Da), indicating the methoxide ligands on the hexavanadate SBUs are fairly labile.

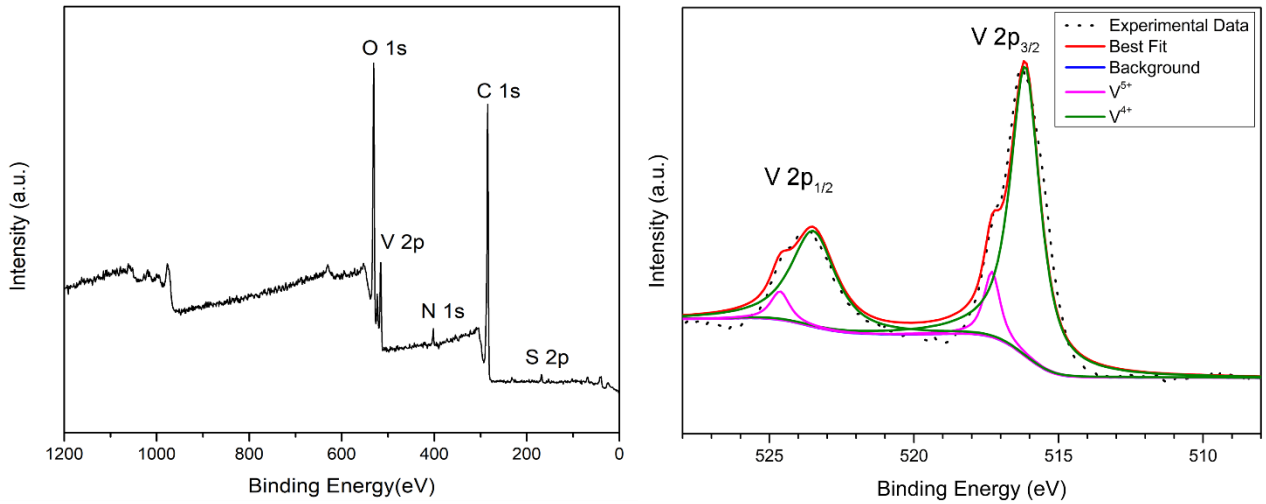


**Fig. S15.** XPS spectrum (left) of **1** and the region (right) for V $2p_{1/2}$ and V $2p_{3/2}$ peaks.

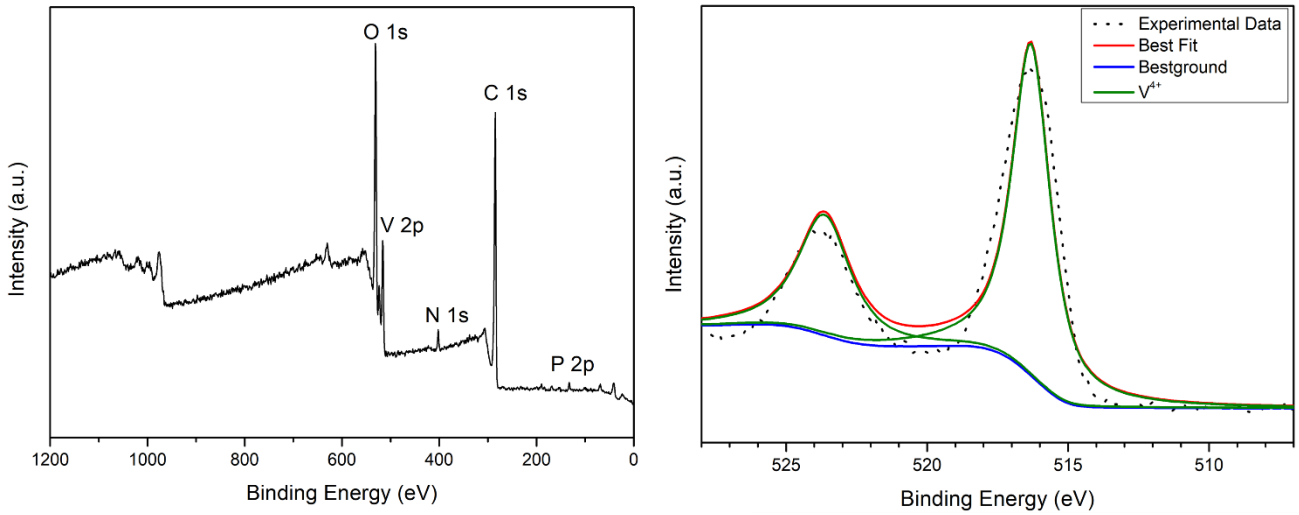


**Fig. S16.** XPS spectrum (left) of **1'** and the region (right) for V $2p_{1/2}$ and V $2p_{3/2}$ peaks.

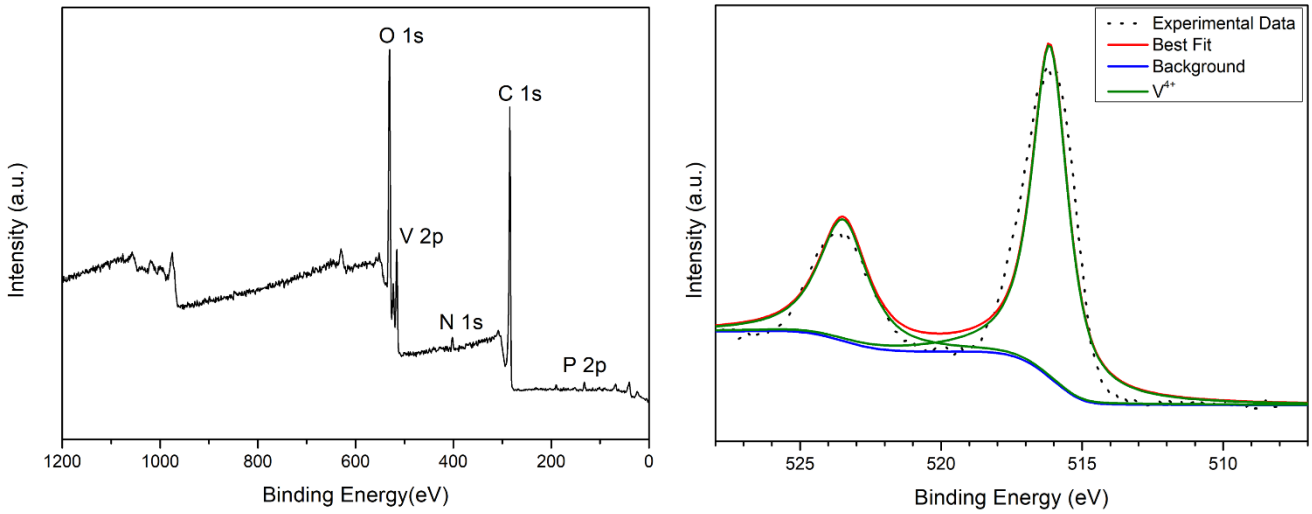


**Fig. S17.** XPS spectrum (left) of **2** and the region (right) for V $2p_{1/2}$ and V $2p_{3/2}$ peaks.

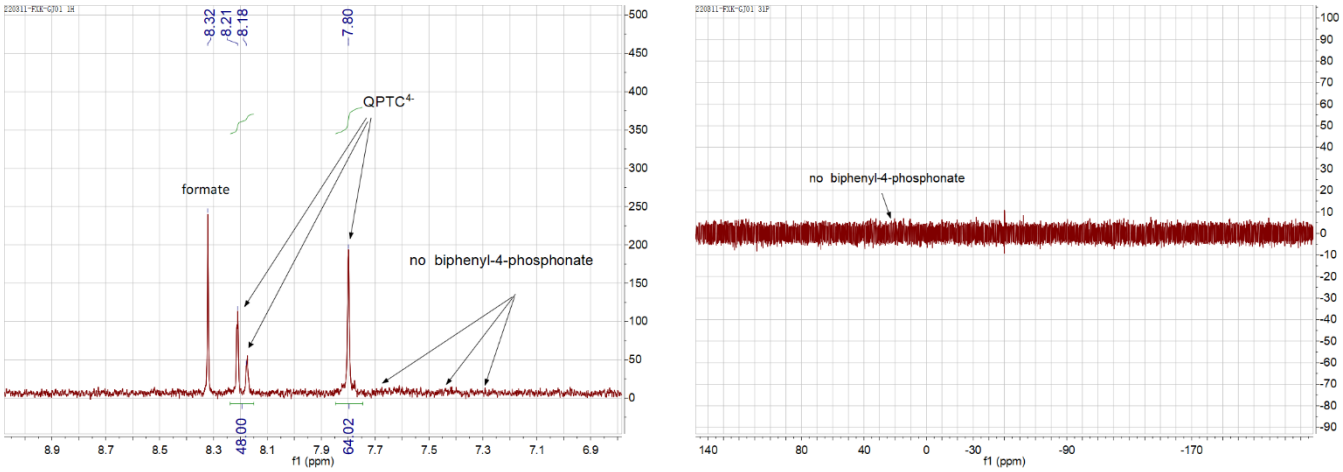


**Fig. S18.** $^{1}$H NMR (left) and $^{31}$P NMR (right) spectra of a base-digested sample of the crystalline product after attempting to post-functionalize MOP **1** with biphenyl-4-phosphonic acid (400 MHz, NaOD/$D_2O$, 293 K). The results confirmed that no sulfate ions in its {$V_6S$} SBUs was replaced by phosphonates, and the product was still MOP **1**.

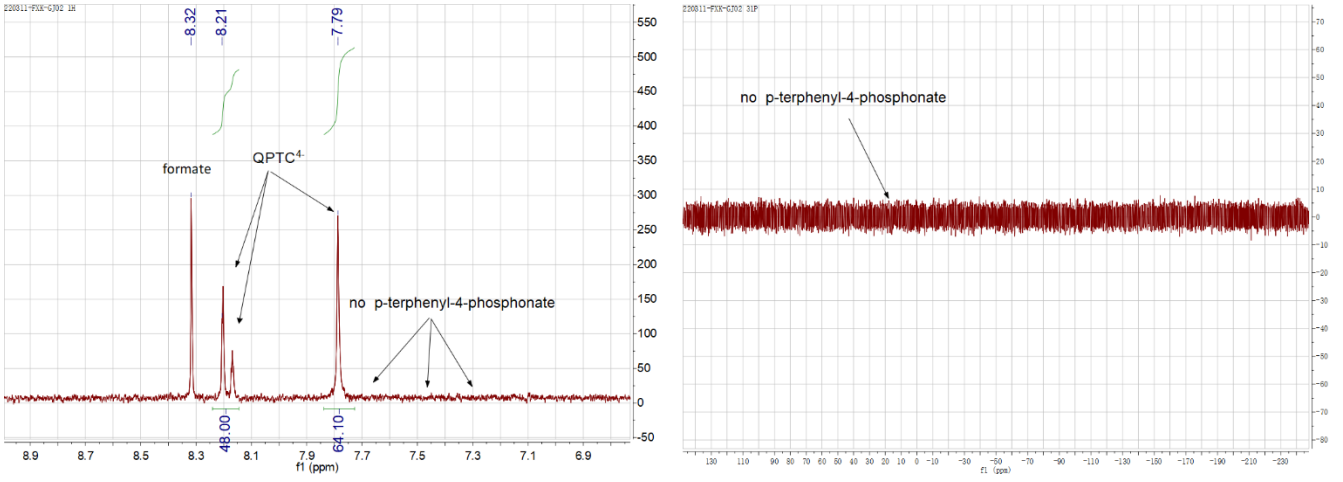


**Fig. S19.** $^{1}$H NMR (left) and $^{31}$P NMR (right) spectra of a base-digested sample of the crystalline product after attempting to post-functionalize MOP **1** with *p*-terphenyl-4-phosphonic acid (400 MHz, NaOD/$D_2O$, 293 K). The results confirmed that no sulfate ions in its {$V_6S$} SBUs was replaced by phosphonates, and the product was still MOP **1**.

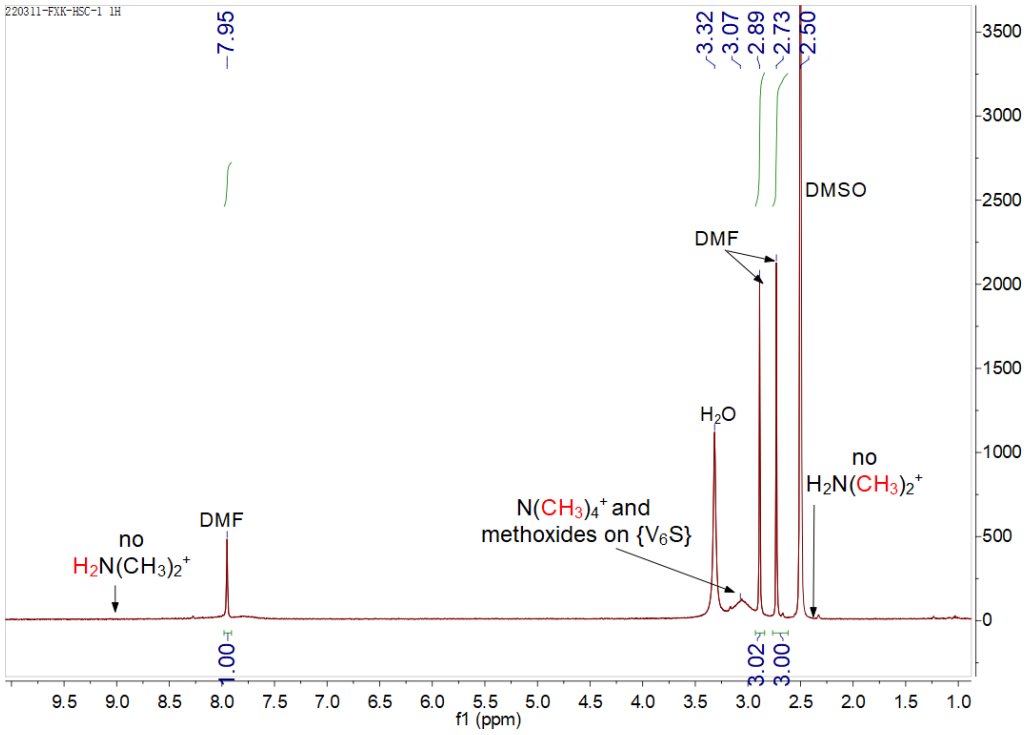


**Fig. S20.** Solution $^{1}$H NMR of compound **1** dissolved in $d_6$-DMSO.

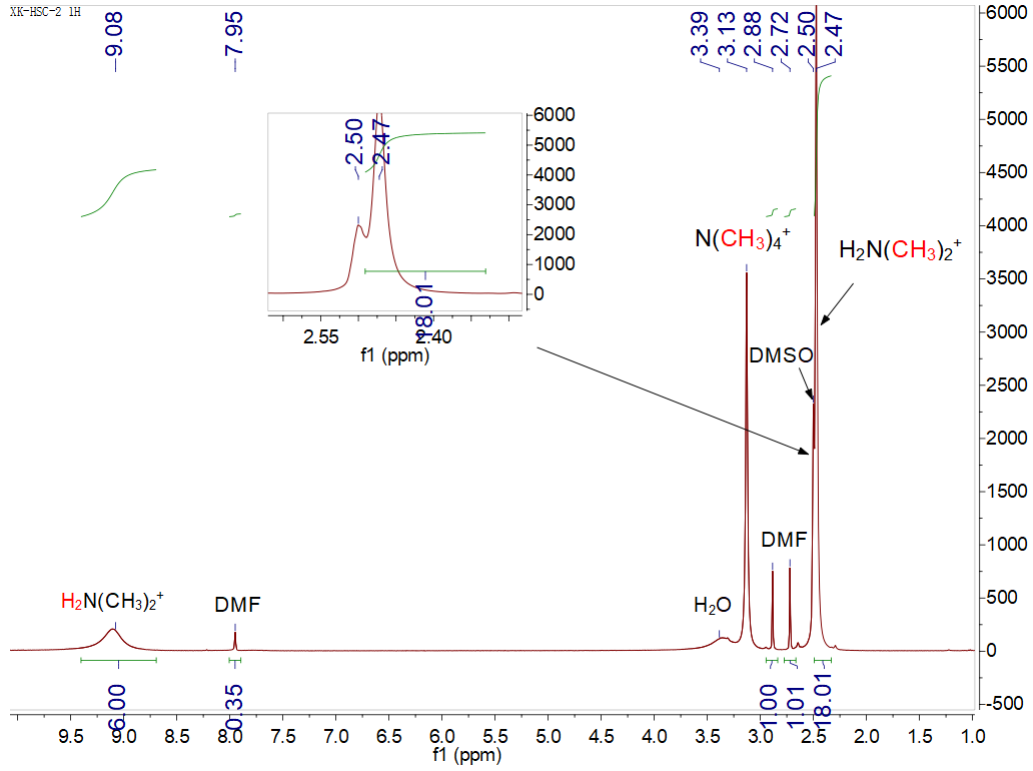


**Fig. S21.** Solution $^{1}$H NMR of compound **1** dissolved in $d_6$-DMSO, with added $TMA^{+}Cl^{-}$ and $DMA^{+}Cl^{-}$, as references for identifying counter ions.

## Single-Crystal X-Ray Structure Determination

**Table S1. C**rystal data and structure refinement for **1** (CCDC deposit number: 2144006).

| | **1** |
|---|---|
| Empirical formula | $C_{423}H_{697}N_{33}O_{273}S_8V_{54}$ |
| Formula weight | 13620.33 |
| Temperature | 173(2) K |
| Wavelength | 0.71073 Å |
| Crystal system | Triclinic |
| Space group | *P*-1 |
| Unit cell dimensions | $a$ = 20.5891(17) Å $\alpha$ = 113.872(2)°.<br>$b$ = 28.609(2) Å $\beta$ = 92.142(2)°.<br>$c$ = 33.168(3) Å $\gamma$ = 103.627(2)°. |
| Volume | 17168(2) Å$^3$ |
| $Z$ | 1 |
| Density (calculated) | 1.317 Mg/m$^3$ |
| Absorption coefficient | 0.803 mm$^{-1}$ |
| $F$(000) | 7020 |
| Crystal size | 0.600 x 0.600 x 0.300 mm$^3$ |
| Theta range for data collection | 2.141 to 26.433° |
| Index ranges | –25<=h<=25, –35<=k<=35, –41<=l<=41 |
| Reflections collected | 236288 |
| Independent reflections | 70399 [R(int) = 0.0986] |
| Completeness to $\theta$ = 25.242° | 99.8% |
| Absorption correction | Semi-empirical from equivalents |
| Refinement method | Full-matrix least-squares on $F^2$ |
| Data / restraints / parameters | 70399 / 71 / 1728 |
| Goodness-of-fit on $F^2$ | 1.052 |
| Final $R$ indices [$I>2\sigma(I)$] | $R_1$ = 0.1495, $wR_2$ = 0.3398 |
| $R$ indices (all data) | $R_1$ = 0.2529, $wR_2$ = 0.4042 |
| Largest diff. peak and hole | 1.667 and –3.731 e.Å$^{-3}$ |

*$R_1 = \Sigma||F_o| - |F_c||/\Sigma|F_o|$, $wR_2 = [\Sigma[w(F_o^2 - F_c^2)^2]/\Sigma[w(F_o^2)^2]]^{1/2}$

**Table S2.** Crystal data and structure refinement for **1'** (CCDC deposit number: 2144007).

| | **1'** |
|---|---|
| Empirical formula | $C_{463}H_{730}N_{26}O_{239}P_8V_{52}$ |
| Formula weight | 13381.33 |
| Temperature | 220(2) K |
| Wavelength | 0.71073 Å |
| Crystal system | Triclinic |
| Space group | *P*-1 |
| Unit cell dimensions | $a$ = 26.268(2) Å $\alpha$ = 87.768(2)°.<br>$b$ = 27.835(2) Å $\beta$ = 71.483(2)°.<br>$c$ = 30.643(3) Å $\gamma$ = 69.654(2)°. |
| Volume | 19856(3) Å$^3$ |
| $Z$ | 1 |
| Density (calculated) | 1.119 Mg/m$^3$ |
| Absorption coefficient | 0.663 mm$^{-1}$ |
| $F$(000) | 6918 |
| Crystal size | 0.530 x 0.510 x 0.330 mm$^3$ |
| Theta range for data collection | 1.868 to 22.054° |
| Index ranges | –27<=h<=27, –29<=k<=29, –32<=l<=32 |
| Reflections collected | 339784 |
| Independent reflections | 48833 [R(int) = 0.1721] |
| Completeness to $\theta$ = 22.054° | 99.5% |
| Absorption correction | Semi-empirical from equivalents |
| Refinement method | Full-matrix least-squares on $F^2$ |
| Data / restraints / parameters | 48833 / 26 / 1895 |
| Goodness-of-fit on $F^2$ | 1.010 |
| Final $R$ indices [$I>2\sigma(I)$] | $R_1$ = 0.1133, $wR_2$ = 0.2957 |
| $R$ indices (all data) | $R_1$ = 0.2064, $wR_2$ = 0.3927 |
| Largest diff. peak and hole | 1.133 and –0.622 e.Å$^{-3}$ |

*$R_1 = \Sigma||F_o| - |F_c||/\Sigma|F_o|$, $wR_2 = [\Sigma[w(F_o^2 - F_c^2)^2]/\Sigma[w(F_o^2)^2]]^{1/2}$

**Table S3.** Crystal data and structure refinement for **2** (CCDC deposit number: 2144008).

| | **2** |
|---|---|
| Empirical formula | $C_{462}H_{719}N_{29}O_{236}P_8V_{48}$ |
| Formula weight | 13148.50 |
| Temperature | 173(2) K |
| Wavelength | 0.71073 Å |
| Crystal system | Monoclinic |
| Space group | *C*2/*c* |
| Unit cell dimensions | $a$ = 45.210(2) Å $\alpha$ = 90°.<br>$b$ =27.4006(14) Å $\beta$ = 113.9190(10)°.<br>$c$ = 55.215(4) Å $\gamma$ = 90°. |
| Volume | 62525(6) Å$^3$ |
| *Z* | 4 |
| Density (calculated) | 1.397 Mg/m$^3$ |
| Absorption coefficient | 0.786 mm$^{-1}$ |
| *F*(000) | 27224 |
| Crystal size | 0.450 x 0.350 x 0.320 mm$^3$ |
| Theta range for data collection | 2.194 to 21.556° |
| Index ranges | –46<=h<=46, –28<=k<=28, –49<=l<=56 |
| Reflections collected | 172105 |
| Independent reflections | 35874 [R(int) = 0.0507] |
| Completeness to $\theta$ = 21.556° | 99.1% |
| Absorption correction | Semi-empirical from equivalents |
| Refinement method | Full-matrix least-squares on $F^2$ |
| Data / restraints / parameters | 35874 / 52 / 1261 |
| Goodness-of-fit on $F^2$ | 1.051 |
| Final *R* indices [$I>2\sigma(I)$] | $R_1$ = 0.1445, $wR_2$ = 0.4306 |
| *R* indices (all data) | $R_1$ = 0.1828, $wR_2$ = 0.4952 |
| Largest diff. peak and hole | 1.973 and –1.596 e.Å$^{-3}$ |

*$R_1 = \Sigma||F_o| - |F_c||/\Sigma|F_o|$, $wR_2 = [\Sigma[w(F_o^2 - F_c^2)^2]/\Sigma[w(F_o^2)^2]]^{1/2}$

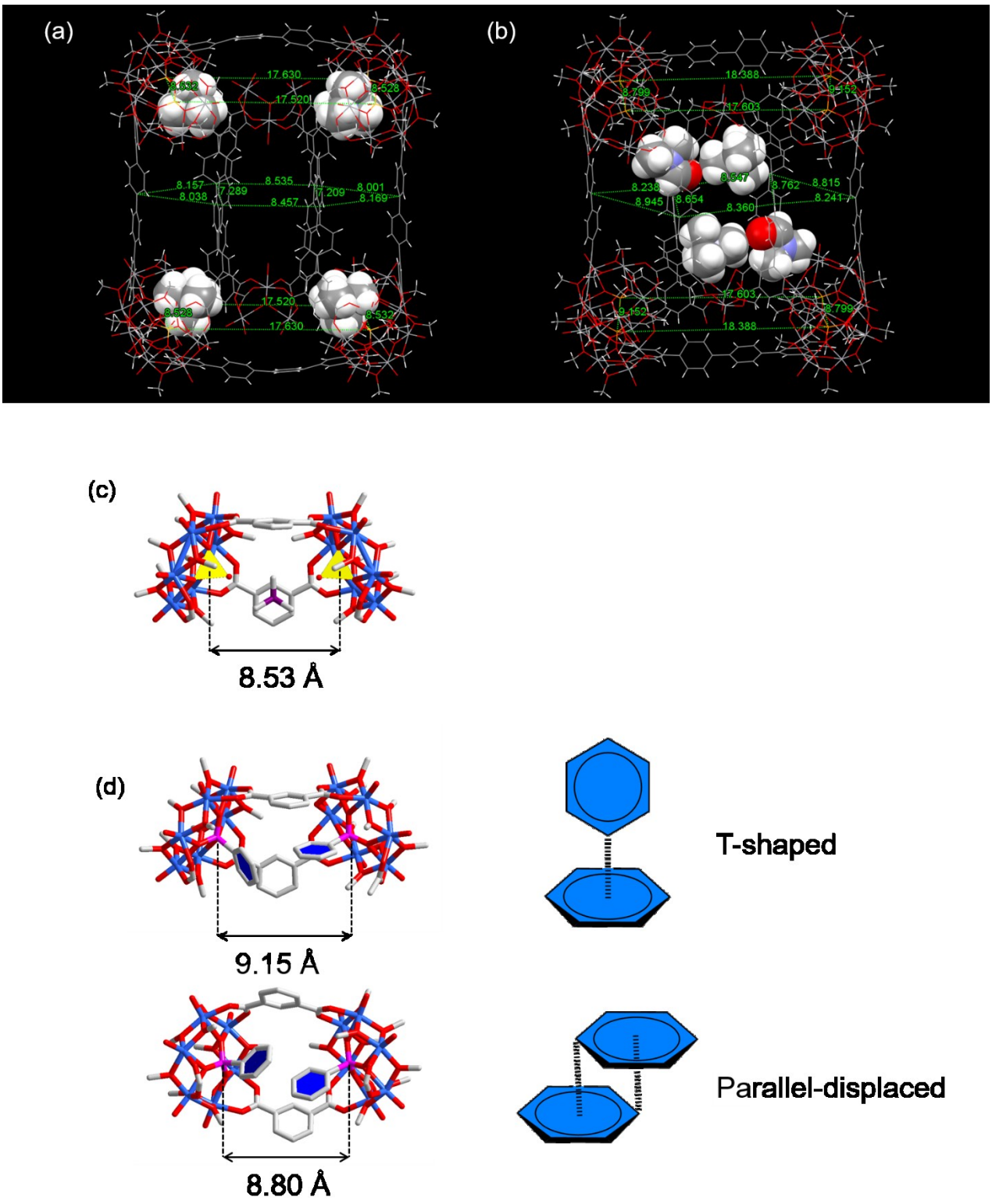


**Fig. S22**. The distances between adjacent hexavanadate clusters (S/P···S/P separations, in Å) and those between adjacent QPTC linkers in **1**(a) and **1'**(b); the distances between adjacent hexavanadate clusters in **1** (c); and pi-pi stacking interactions between the phenyl rings of the phosphonate functional groups in **1'**(d).

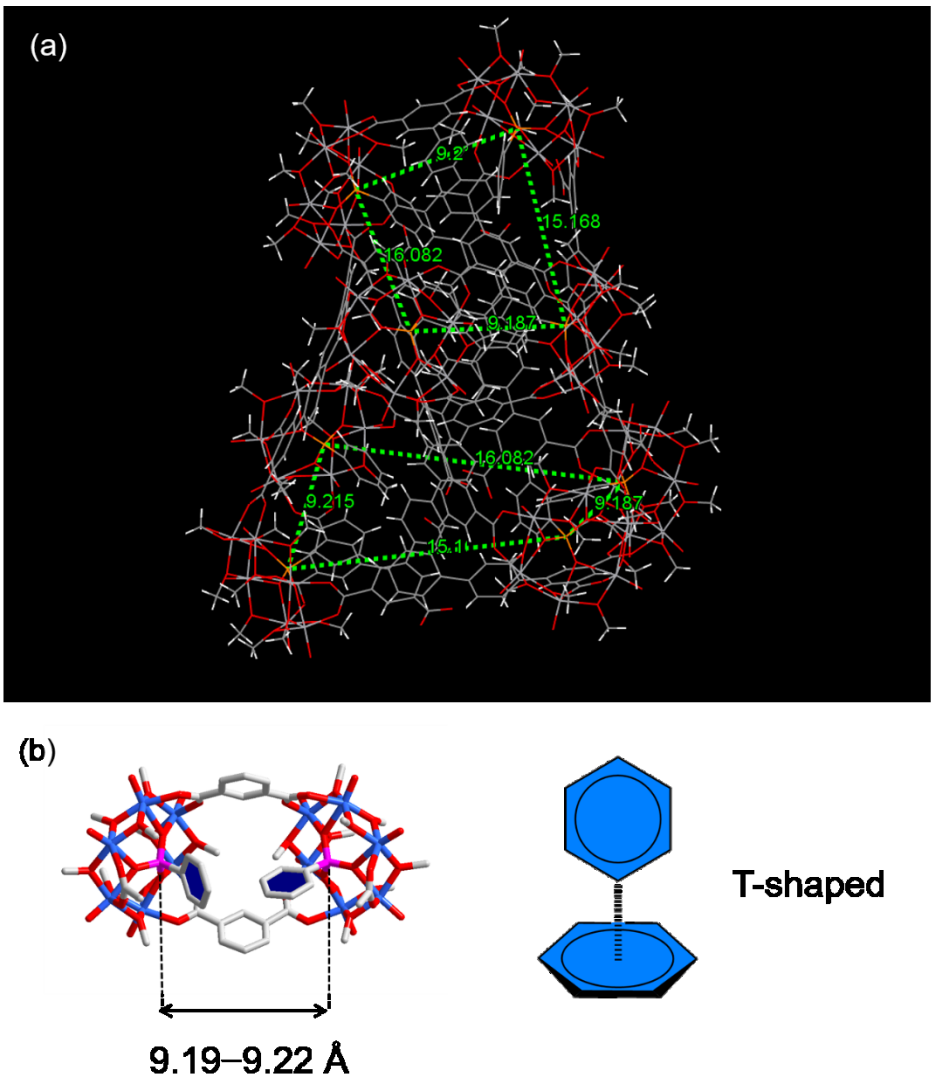


**Fig. S23**. (a) The distances between adjacent hexavanadate clusters (P···P separations) in **2**; (b) pi-pi stacking interactions between the phenyl rings of the phosphonate functional groups in **2**.

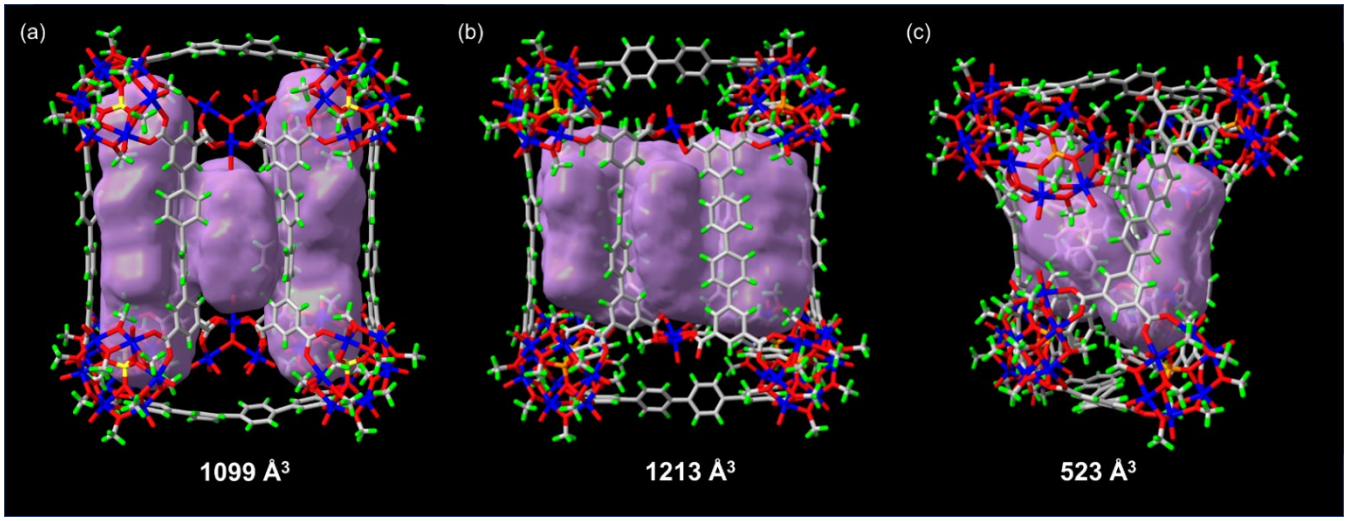


**Fig. S24**. The inner void space of **1**(a), **1'**(b) and **2**(c); cavity volumes were calculated by the 3V program.[S7]

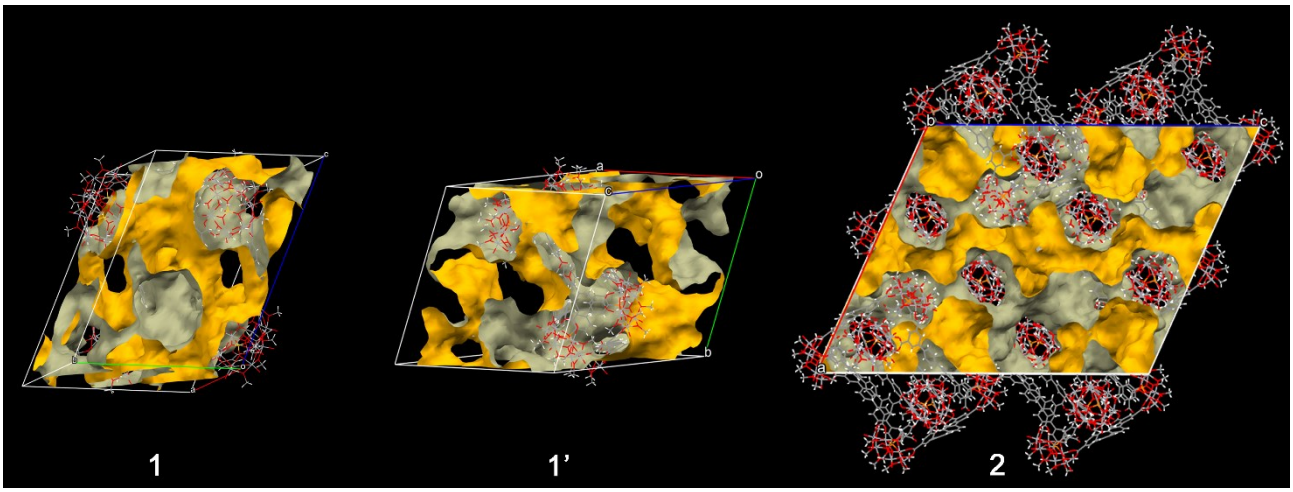


**Fig. S25.** Crystal packing diagrams of **1**, **1'**, and **2** showing the space (in orange) between the MOP molecules, which may be accessed by guests such as MB dye molecules. The void spaces (without counter ions and solvents) between MOP molecules are calculated to be 49.6%, 53.0%, and 38.0% of the cell volumes for **1**, **1'**, and **2**, respectively. (Calculation and drawing were done with CCDC Mercury 2021.2.0. Probe radius, 1.2 Å; grid spacing 0.7 Å; contact surface.)

## Bond Valence Sum (BVS) Calculations:

For determination of the oxidation states of metal centers and the protonation states of oxygen sites, BVS calculations were carried out using the method of I. D. Brown.[S8] The $r_o$ values were taken from the literature[S9] for calculations performed on V.

**Table S4.** BVS calculations for V sites in **1**.

| Vanadium Atoms | BVS | | | Assigned Oxidation States |
|---|---|---|---|---|
| | V(III) | V(IV) | V(V) | |
| V1 | 3.791 | **3.934** | 4.387 | IV |
| V2 | 3.909 | **4.066** | 4.523 | IV |
| V3 | 3.741 | **3.885** | 4.329 | IV |
| V4 | 3.898 | **4.046** | 4.510 | IV |
| V5 | 3.915 | **4.061** | 4.530 | IV |
| V6 | 3.821 | **3.962** | 4.422 | IV |
| V7 | 3.792 | **3.940** | 4.388 | IV |
| V8 | 3.816 | **3.968** | 4.415 | IV |
| V9 | 3.849 | **3.989** | 4.454 | IV |
| V10 | 3.888 | **4.031** | 4.499 | IV |
| V11 | 3.986 | **4.138** | 4.613 | IV |
| V12 | 3.932 | **4.075** | 4.550 | IV |
| V13 | 3.863 | **4.007** | 4.470 | IV |
| V14 | 3.784 | **3.938** | 4.379 | IV |
| V15 | 3.747 | **3.893** | 4.336 | IV |
| V16 | 3.840 | **3.991** | 4.443 | IV |
| V17 | 3.744 | **3.884** | 4.333 | IV |
| V18 | 3.786 | **3.932** | 4.381 | IV |
| V19 | 3.917 | **4.066** | 4.532 | IV |
| V20 | 3.759 | **3.907** | 4.350 | IV |
| V21 | 3.879 | **4.023** | 4.489 | IV |
| V22 | 3.833 | **3.979** | 4.436 | IV |
| V23 | 3.714 | **3.863** | 4.298 | IV |
| V24 | 3.845 | **3.990** | 4.449 | IV |
| V25 | 4.131 | 4.316 | **4.780** | V |
| V26 | 4.279 | 4.486 | **4.952** | V |
| V27 | 4.104 | 4.269 | **4.749** | V |

**Table S5.** BVS calculations for V sites in **1'**.

| Vanadium Atoms | BVS | | | Assigned Oxidation States |
|---|---|---|---|---|
| | V(III) | V(IV) | V(V) | |
| V1 | 3.975 | **4.118** | 4.600 | IV |
| V2 | 3.767 | **3.911** | 4.359 | IV |
| V3 | 3.913 | **4.063** | 4.528 | IV |
| V4 | 3.745 | **3.898** | 4.334 | IV |
| V5 | 3.851 | **4.000** | 4.456 | IV |
| V6 | 3.788 | **3.940** | 4.384 | IV |
| V7 | 3.875 | **4.019** | 4.483 | IV |
| V8 | 3.770 | **3.911** | 4.362 | IV |
| V9 | 3.888 | **4.044** | 4.499 | IV |
| V10 | 3.909 | **4.051** | 4.523 | IV |
| V11 | 3.793 | **3.947** | 4.389 | IV |
| V12 | 3.777 | **3.925** | 4.370 | IV |
| V13 | 3.818 | **3.962** | 4.418 | IV |
| V14 | 3.800 | **3.949** | 4.397 | IV |
| V15 | 3.851 | **4.005** | 4.456 | IV |
| V16 | 3.968 | **4.112** | 4.591 | IV |
| V17 | 3.802 | **3.948** | 4.399 | IV |
| V18 | 3.799 | **3.951** | 4.396 | IV |
| V19 | 3.711 | **3.860** | 4.294 | IV |
| V20 | 3.815 | **3.961** | 4.415 | IV |
| V21 | 3.876 | **4.024** | 4.486 | IV |
| V22 | 3.786 | **3.939** | 4.381 | IV |
| V23 | 3.783 | **3.923** | 4.377 | IV |
| V24 | 3.879 | **4.034** | 4.489 | IV |
| V25 | 3.826 | **3.962** | 4.428 | IV |
| V26 | 3.792 | **3.922** | 4.388 | IV |

**Table S6.** BVS calculations for V sites in **2**.

| Vanadium Atoms | BVS | | | Assigned Oxidation States |
|---|---|---|---|---|
| | V(III) | V(IV) | V(V) | |
| V1 | 3.822 | **3.969** | 4.422 | IV |
| V2 | 3.748 | **3.895** | 4.337 | IV |
| V3 | 3.868 | **4.013** | 4.476 | IV |
| V4 | 3.746 | **3.896** | 4.335 | IV |
| V5 | 3.724 | **3.864** | 4.309 | IV |
| V6 | 3.835 | **3.983** | 4.437 | IV |
| V7 | 3.725 | **3.885** | 4.310 | IV |
| V8 | 3.704 | **3.845** | 4.286 | IV |
| V9 | 3.867 | **4.022** | 4.475 | IV |
| V10 | 4.111 | **4.263** | 4.757 | IV |
| V11 | 3.839 | **3.986** | 4.443 | IV |
| V12 | 3.706 | **3.850** | 4.288 | IV |
| V13 | 3.784 | **3.920** | 4.378 | IV |
| V14 | 3.779 | **3.923** | 4.373 | IV |
| V15 | 3.841 | **4.005** | 4.445 | IV |
| V16 | 3.759 | **3.902** | 4.349 | IV |
| V17 | 3.900 | **4.044** | 4.513 | IV |
| V18 | 3.817 | **3.958** | 4.417 | IV |
| V19 | 3.749 | **3.898** | 4.338 | IV |
| V20 | 3.737 | **3.888** | 4.325 | IV |
| V21 | 3.826 | **3.972** | 4.427 | IV |
| V22 | 3.795 | **3.943** | 4.391 | IV |
| V23 | 3.803 | **3.958** | 4.401 | IV |
| V24 | 3.761 | **3.903** | 4.352 | IV |

**Table S7**. BVS calculations for selected oxygen atoms in **1**, **1'**, and **2**.

| Compounds | Selected Oxygen Atoms | BVS | Assigned Protonation Levels |
|---|---|---|---|
| **1** | O109 | 2.153 | O |
| | O110 | 0.337 | $H_2O$ |
| | O111 | 0.617 | $H_2O$ |
| | O112 | 1.214 | OH |
| | O113 | 1.552 | O |
| | O114 | 1.802 | O |
| | O115 | 0.958 | OH |
| | O116 | 0.633 | $H_2O$ |
| **1'** | O105 | 2.000 | O |
| | O106 | 2.150 | O |
| | O107 | 1.561 | O |
| | O108 | 1.539 | O |

## References:


S1 X. Lin, I. Telepeni, A. J. Blake, A. Daily, C. M. Brown, J. M. Simmons, M. Zoppi, G. S. Walker, K. M. Thomas, T. J. Mays, P. Hubberstey, N. R. Champness and M. Schroder, *J. Am. Chem. Soc.* 2009, **131**, 2159–2171.

S2 (a) Y.-T. Zhang, X.-L. Wang, S.-B. Li, Y.-R. Gong, B.-Q. Song, K.-Z. Shao and Z.-M. Su, *Chem. Commun.*, 2016, **52**, 9632–9635; (b) Y.-T. Zhang, S.-B. Li, X.-L. Wang, Y.-R. Gong, K.-Z. Shao and Z.-M. Su, *Dalton Trans.*, 2016, **45**, 14898–14901; (c) Y.-R. Gong, W.-C. Chen, L. Zhao, K.-Z. Shao, X.-L. Wang and Z.-M. Su, *Dalton Trans.*, 2018, **47**, 12979–12983; (d) Y. Gong, Y. Zhang, C. Qin, C. Sun, X. Wang and Z. Su, *Angew. Chem., Int. Ed.*, 2019, **58**, 780–784; (e) Y. Gong, C. Qin, Y. Zhang, C. Sun, Q. Pan, X. Wang and Z. Su, *Angew. Chem.*, *Int. Ed.* 2020, **59***,* 22034–22038.

S3 (a) X. Hang, B. Liu, X. Zhu, S. Wang, H. Han, W. Liao, Y. Liu and C. Hu, *J. Am. Chem. Soc.*, 2016, **138**, 2969–2972; (b) J.-Q. Liu, J. Wu, J. Wang, L. Lu, C. Daiguebonne, G. Calvez, O. Guillou, H. Sakiyama, N. S. Weng and M. Zeller, *RSC Adv.*, 2014, **4**, 20605–20611.

S4 G. M. Sheldrick, *Acta Crystallogr.* 2015, **A71**, 3–8.

S5 G. M. Sheldrick, *Acta Crystallogr.* 2008, **A64**, 112–122.

S6 A. L. Spek, *Acta Crystallogr.* 2015, **C71**, 9–18.

S7 N. R. Voss and M. Gerstein, *Nucleic Acids Res*, 2010, **38**, W555−W562.

S8 I. D. Brown and D. Altermatt, *Acta Crystallogr. Sect. B*, 1985, **41**, 244–247.

S9 W. Liu and H. H. Thorp, *Inorg. Chem.* 1993, **32**, 4102–4105.